Materials Transactions, Vol. 50, No. 6 (2009) pp. 1300 to 1303
Special Issue on Joining Technology for New Metallic Glasses and Inorganic Materials

Friction Stir Welding of $Zr_{55}Cu_{30}Ni_5Al_{10}$ Bulk Metallic Glass

Young Su Ji[1], Hidetoshi Fujii[1,*], Yufeng Sun[1], Masakatsu Maeda[1], Kazuhiro Nakata[1], Hisamichi Kimura[2], Akihisa Inoue[2] and Kiyoshi Nogi[1]

[1]*Joining and Welding Research Institute, Osaka University, Ibaraki 567-0047, Japan*
[2]*Institute for Materials Research, Tohoku University, Sendai 980-8577, Japan*

A $Zr_{55}Cu_{30}Ni_5Al_{10}$ bulk metallic glass plate was successfully welded below its crystallization temperature by friction stir welding. The flash formation and heat concentration at the shoulder edge was minimized using a wider tool with the shoulder surface recessed by an angle of 3°. To evaluate the crystallization of the weld, the microstructure and mechanical properties were analyzed using DSC, XRD, TEM, and micro-hardness. As a result, it was found that the amorphous structure and original mechanical properties were maintained throughout the entire joint. [doi:10.2320/matertrans.ME200806]

(Received December 3, 2008; Accepted March 31, 2009; Published May 25, 2009)

Keywords: *annealing, bulk metallic glass, friction stir welding*

1. Introduction

Bulk metallic glasses (BMGs) in various kinds of alloy systems have been discovered since the $Au_{75}Si_{25}$ amorphous alloy was first produced by Duwez using a rapid solidification technique in 1960.[1)] BMGs have excellent properties including high strength, good wear resistance, good magnetic properties, corrosion resistance, good forming ability, etc.,[2–6)] which can be attributed to the long range disordered structure on an atomic scale. Accordingly, BMGs are considered to be the next generation materials, and active research studies of them are now in progress. However, size limitation is still a long-standing problem for engineering applications as structural materials because a high cooling rate (1∼100 k/s) is usually necessary to produce the BMGs. Although there are some alloy families like the Zr-, La, Pd-based BMGs exhibiting a good glass forming ability, sufficient to fabricate BMGs of several centimeter diameter, their alloy composition was localized in a very narrow range. In order to solve this problem, several recent studies on the joining of BMGs have been done.[7–15)] The feasibility of friction welding,[7–9,11,12)] pulse-current welding,[12)] spark welding,[13)] electron-beam welding,[14)] and explosive welding[15)] methods for some BMGs has been demonstrated. Friction stir welding was invented at The Welding Institute (TWI) of the UK in 1991. Friction stir welding is a new solid-state joining process. This joining technique is energy efficient, environmentally friendly and versatile. Active research studies of friction stir welding are now in progress.[16)] Wang *et al.*[17)] reported that the $Zr_{55}Cu_{30}Ni_5Al_{10}$ bulk metallic glass and 7075 aluminum alloy were successfully welded using friction stir welding. However, the friction stir welding of BMG to itself has not been successfully performed.

In this study, the $Zr_{55}Cu_{30}Ni_5Al_{10}$ bulk metallic glass was joined using friction stir welding. The mechanical properties and microstructure of the welded joints were then investigated.

*Corresponding author, E-mail: fujii@jwri.osaka-u.ac.jp

2. Experimental Procedure

A $Zr_{55}Cu_{30}Ni_5Al_{10}$ bulk metallic glass master alloy ingot was made by arc melting using high purity Zr (99.9%), Cu (99.9%), Ni (99.9%) and Al (99.9%), and then fully amorphous specimens of 75 × 50 × 2 mm metallic glass square plates were prepared by copper mold casting in an Ar atmosphere. The stir-in-plate and butt welding experiments of the $Zr_{55}Cu_{30}Ni_5Al_{10}$ bulk metallic glass were performed using a position-controlled FSW machine. The tool, which was made of SKD61, had a 25 mm shoulder diameter, 5 mm probe diameter, and 2 mm probe length with a 3° recessed shoulder surface. The probe was the screw-type and the tool was not tilted. The tool rotation speed was varied between 80 and 150 rpm to control the heat input, while the traveling speed was fixed at 100 mm/min.

The thermal properties of the $Zr_{55}Cu_{30}Ni_5Al_{10}$ bulk metallic glass joints were measured by differential scanning calorimetry (DSC, Bruker, DSC 3300SA) at the heating rate of 20 K/min in an flowing Ar gas atmosphere. The phase identification and microstructures of the specimens were examined by X-ray diffraction (XRD) and transmission electron microscopy (TEM). The XRD analysis was conducted (Bruker, AXS D8 DISCOVER) using Co-Kα radiation. The samples for the TEM observations were prepared using twin-jet electrolytic polishing in a solution with a mixed ratio of $HClO_4 : C_2H_5O_4 = 1 : 9$. The TEM observations were done at 200 kV using a Hitachi H800T. The Vickers micro-hardness (HV) values were determined using a (Akashi, AAV 501) digital microhardness tester with the testing load of 100 gf (= 0.98 N).

3. Results and Discussion

3.1 Tool shape

In this study, in order to minimize any flash formation, a tool with the wider shoulder diameter of 25 mm was used, though a shoulder of about 12 mm diameter is generally used to weld a workpiece of 2 mm thickness. The shoulder surface of the tool was recessed by an angle of 0∼10°. As shown in Fig. 1(a), when the recessed angle of the shoulder surface

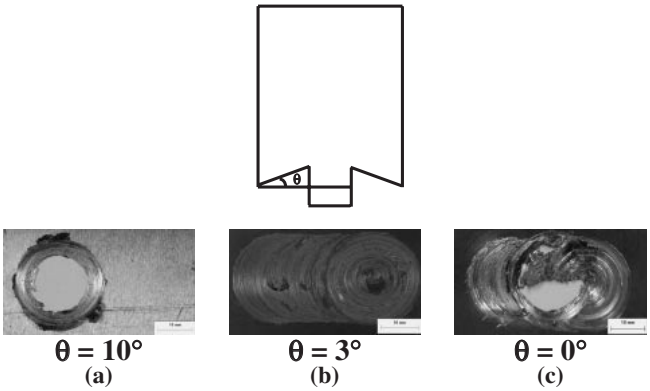

Fig. 1 Appearance of the friction stir welded specimen at 150 rpm and 100 mm/min with various recessed angles of the shoulder surface: (a) 10°, (b) 3°, and (c) 0°.

is 10°, the heat input is concentrated at the shoulder edge. As a result, the surface becomes pitted at the shoulder edge. When the angle of the recessed shoulder surface is 0° as shown in Fig. 1(c), much flash is formed. However, when the recessed angle of the shoulder surface is 3°, as shown in Fig. 1(b), a comparatively good surface is obtained. Based on these results, the recessed angle of the shoulder was finally fixed at 3°.

Figure 2 shows the surface appearances of the stir-in-plate specimens of the $Zr_{55}Cu_{30}Ni_5Al_{10}$ bulk metallic glass obtained at different rotation speeds. When the rotation speed is 80 rpm as shown in Fig. 2(a), defects are formed on the surface, because the heat input is insufficient. When the rotation speed is between 100 rpm and 150 rpm, no large defects or cracks are formed in the stir zone surface, as shown in Figs. 2(b) and (c).

3.2 Microstructure and mechanical properties of stir-in-plate specimens

Figure 3 shows the XRD patterns of the base material and the center of the stir zones of the stir-in-plate specimens. As shown in Fig. 3, the XRD patterns of the base material and stir zone show only broad peaks, the typical feature of an amorphous structure. This result suggests that the temperature of the stir zone during the welding was below the crystallization temperature although a precise temperature measurement is necessary to determine the temperature change in the stir zone during the welding. At 170 rpm, on the other hand, some weak crystalline diffraction peaks were found superimposed on the broad peak, as shown in Fig. 3(d). This suggests that crystallization took place in the stir zone at 170 rpm. Therefore, the temperature of the stir zone during the stir-in-plate exceeded the crystallization temperature.

Figure 4 shows the hardness distribution at the center of a cross section perpendicular to the welding direction of the stir-in-plate specimens. Although a crystallization behavior was observed at the rotation speed of 170 rpm as suggested by curve(d) in Fig. 3, there is no significant change in hardness between the base material and stir zone, as shown in Fig. 4. The average values of the hardness in the base material and stir zone are 525HV. Therefore, it can be considered that the crystallization at 170 rpm was only limited.

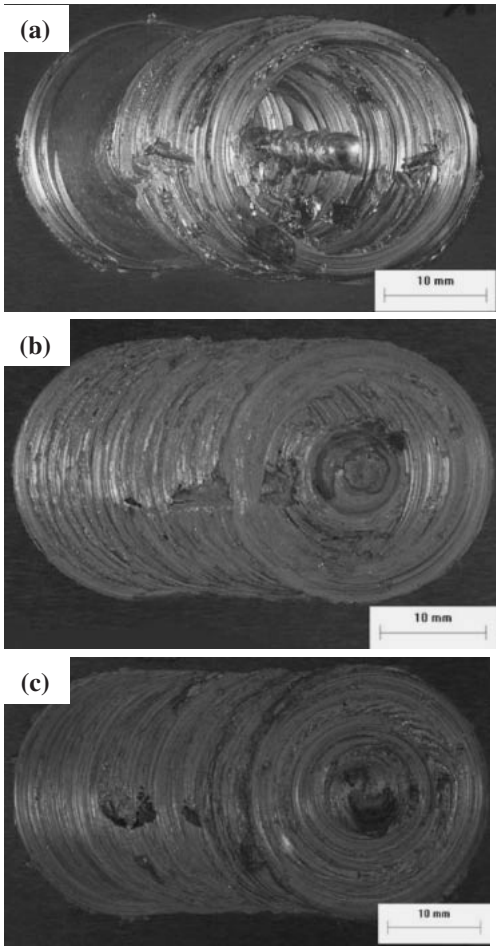

Fig. 2 Macroscopic overview of the stir-in-plate welds of the $Zr_{55}Cu_{30}Al_{10}Ni_5$ bulk metallic glass at the rotation speeds of (a) 80 rpm, (b) 100 rpm, and (c) 150 rpm.

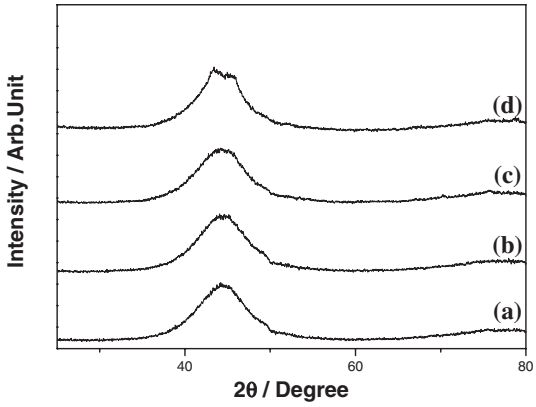

Fig. 3 X-ray diffraction patterns of base material and stir zone: (a) base material, (b) $R = 100$ rpm, (c) $R = 150$ rpm, and (d) $R = 170$ rpm.

Figure 5 shows the DSC results of the specimens cut from the base material and the center. The heating rate of the DSC measurement was 20 K/min. The glass transition temperature (T_g), crystallization temperature (T_x), the peak temperature and the super-cooled liquid region range ($\Delta T = T_x - T_g$) are about 675, 755, 767 and 80 K, respectively. As shown in Fig. 5, exothermic peaks are clearly observed at the rotation speed of 100 rpm without any shift in the T_g and T_x from that of the base metal, indicating that no

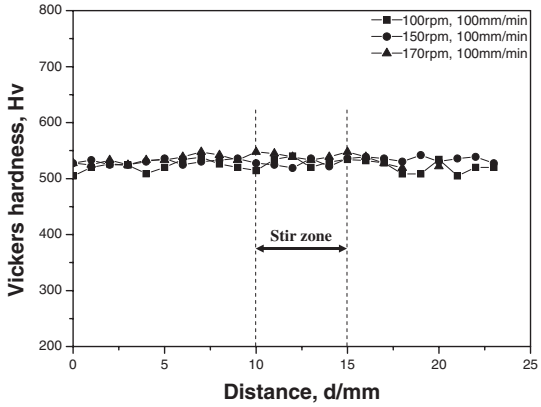

Fig. 4 Hardness distribution on a cross section perpendicular to the welding direction.

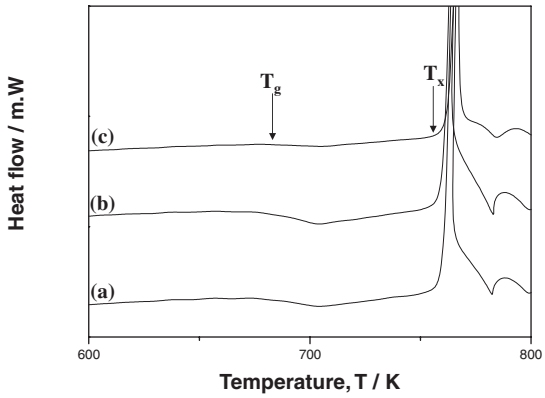

Fig. 5 DSC result (heating rate = 20 K/min) of the base material and stir zone: (a) base material, (b) $R = 100$ rpm, and (c) $R = 150$ rpm.

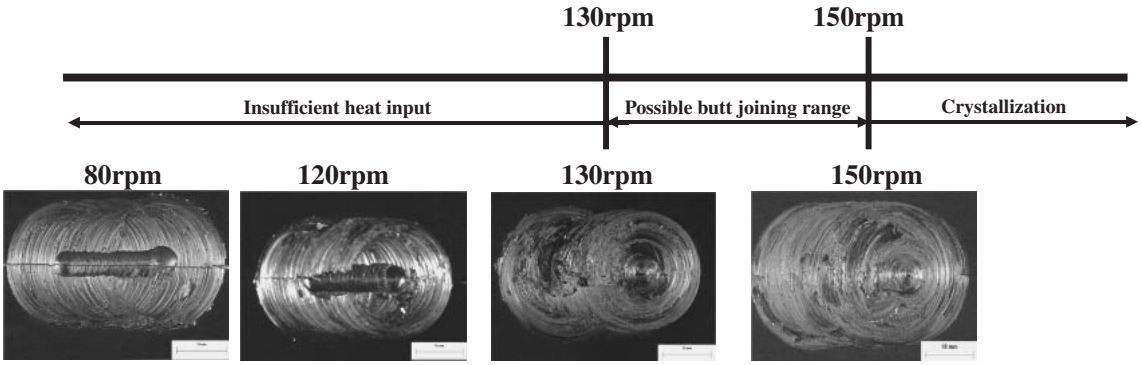

Fig. 6 Possible butt joining range and surface appearances.

crystallization occurred. However, at 150 rpm, a decrease in the area of the exothermic peaks are observed (DSC curve (c) in Fig. 5), suggesting that a small amount of crystallization occurred at 150 rpm.

No significant oxidation of the stir zone sample was observed using the optical microscope, SEM or TEM. Therefore, the oxidation does not seem to have a significant effect on the microstructure and the mechanical properties of the joints under these welding conditions.

3.3 Microstructure and mechanical properties of butt joints

Figure 6 shows the surface appearances of the butt joints of the $Zr_{55}Cu_{30}Ni_5Al_{10}$ bulk metallic glass specimens for various rotation speeds. Although defects are observed on the surface at 80 to 120 rpm, joints with sound surface appearances are obtained at 130–150 rpm. In order to produce a sound butt weld, a greater amount of heat is necessary due to the presence of a gap and contamination at the interface. Accordingly, an increase in the rotation speed is necessary when compared to the stir-in-plate FSW. On the other hand, the surfaces of the specimen come in direct contact with the shoulder during the friction stir welding. Accordingly, the effect of the interface on the soundness of the welds is low for the upper limit of the rotation speed, because the upper limit is determined by the highest temperature in the stir zone. As a result, as shown in Fig. 6, the possible range of the rotation speed to obtain sound FS welds free from any significant crystallization for butt joining becomes quite narrow.

Figure 7 shows the DSC results of specimens cut from the base material and the center of the stir zone of the butt joints. As shown in Fig. 7, exothermic peaks are clearly observed for the butt weld without any shift in the T_g and T_x from that of the base material at $R = 130$ rpm. However, at $R = 150$ rpm, the exothermic peak areas decreased and slightly shifted to a higher temperature (DSC curve (c), in Fig. 7). The same crystallization behaviors were observed in the DSC results shown in Fig. 5 and Fig. 7.

Figure 8 shows the hardness distribution in the center of the cross section perpendicular to the welding direction of the butt joints. As shown in Fig. 8, no significant change in hardness between the base material and stir zone occurred at 130 rpm. However, a large increase in hardness was observed at 150 rpm. This result suggests that the temperature of the stir zone during the friction stir welding exceeded the crystallization temperature.

Figure 9 shows the bright-field TEM images and corresponding selected-area-diffraction (SAD) patterns of the base material (a) and the centers of the stir zones of the butt welds (b), (c). As shown in Figs. 9(a) and (b), no crystalline particles were observed in the bright-field images of the base material and stir zone at $R = 130$ rpm. These results support the conclusion that the base material and stir zone at 130 rpm are homogeneous and amorphous. However, as shown in Fig. 9(c), nanocrystalline areas were observed in the stir zone at 150 rpm. In this case, the temperature of the stir zone exceeded the crystallization temperature during the friction stir welding.

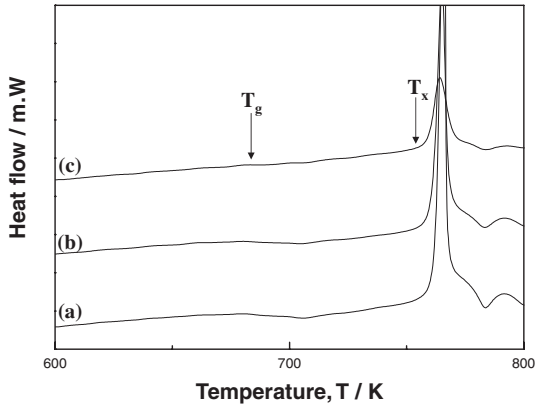

Fig. 7 DSC result (heating rate = 20 K/min) of the base material and stir zone: (a) Base material, (b) $R = 130$ rpm, and (c) $R = 150$ rpm.

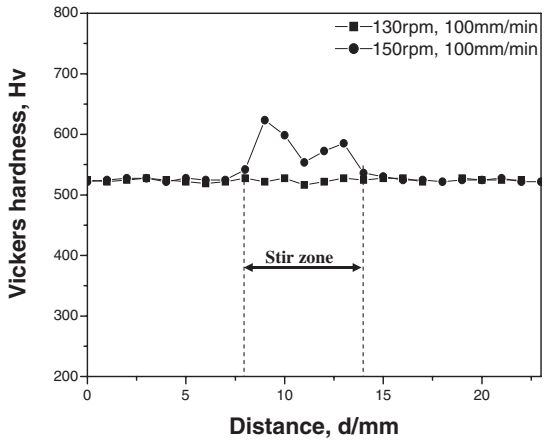

Fig. 8 Hardness distribution of a cross section perpendicular to the welding direction.

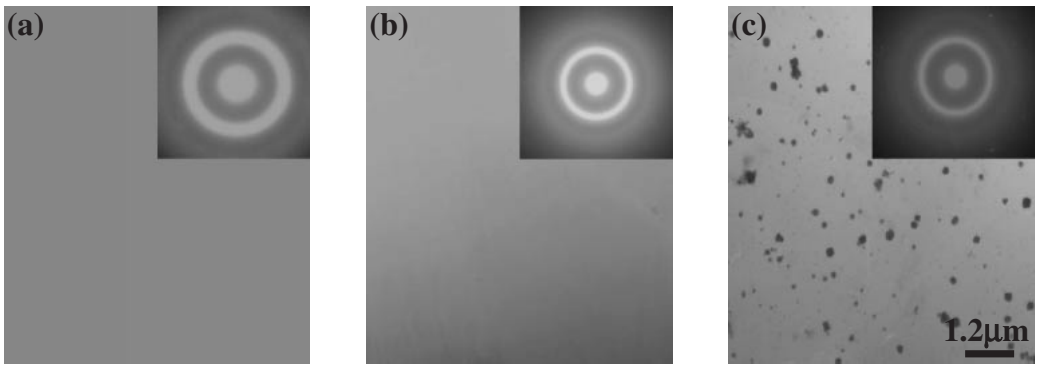

Fig. 9 TEM images of base material and stir zone: (a) base material, (b) $R = 130$ rpm, 100 mm, and (c) $R = 150$ rpm.

4. Conclusions

The $Zr_{55}Cu_{30}Ni_5Al_{10}$ bulk metallic glass was welded by friction stir welding. The obtained results are summarized as follows:

(1) The $Zr_{55}Cu_{30}Ni5Al_{10}$ bulk metallic glass was successfully welded without crystallization by friction stir welding under suitable welding conditions.

(2) The flash formation was minimized using a tool with the wider shoulder diameter of 25 mm, and the excessive heat concentration at the shoulder edge was prevented by using the shoulder surface with a 3° recessed angle.

(3) Observations of the microstructure and mechanical properties of the welded joints showed that the amorphous structure and original mechanical properties of the metallic glass could be maintained under suitable welding conditions.

Acknowledgments

The authors wish to acknowledge the financial support by a Grant-in-Aid for the Cooperative Research Project of Nationwide Joint-Use Research Institutes on Development Base of Joining Technology for New Metallic Glasses and Inorganic Materials, "Priority Assistance of the Formation of Worldwide Renowned Centers of Research-The Global COE Programs (Project: Center of Excellence for Advanced Structural and Functional Materials Design) from the Ministry of Education, Culture, Sports, Science and Technology, Japan and Grant-in-Aid for Science Research from the Japan Society for the Promotion of Science and Technology of Japan.

REFERENCES

1) W. Klement Jr, R. H. Willens and P. Duwez: Nature **187** (1960) 869–870.
2) A. Inoue: Acta Mater. **48** (2000) 279–306.
3) W. L. Johnson: MRS Bulletin **10** (1999) 42–56.
4) S. J. Pang, T. Zhang, K. Asami and A. Inoue: Corrosion Sci. **44** (2002) 1847–1856.
5) W. H. Wang, C. Dong and C. H. Shek: Mater. Sci. Eng. R **44** (2004) 45–89.
6) T. A. Waniuk, R. Busch, A. Masuhr and W. L. Johnson: Acta Mater. **46** (1998) 5229–5236.
7) C. H. Wong and C. H. Shek: Scr. Mater. **49** (2003) 393–397.
8) H. S. Shin, H. Y. Choi and J. S. Park: Adv. Mater. Sci. **18** (2008) 104–106.
9) Y. Kawamura, T. Shoji and Y. Ohno: J Non-Cryst Solid **317** (2003) 152–157.
10) K. X. Liu, W. D. Liu, J. T. Wang, H. H. Yan, X. J. Li, Y. J. Huang, X. S. Wei and J. Shen: Appl. Phys. Lett. **93** (2008) 081918.
11) Y. Kawamura and Y. Ohno: Scr. Mater. **45** (2001) 279–285.
12) Y. Kawamura and Y. Ohno: Mater. Trans. **42** (2001) 717–719.
13) Y. Kawamura and Y. Ohno: Scr. Mater. **45** (2001) 127–132.
14) J. H. Kim and Y. Kawamura: Mater. Proc. Tech. **207** (2008) 112–117.
15) Y. Kawamura, Y. Ohno and A. Chiba: Mater. Sci. Forum **553** (2002) 386–388.
16) R. S. Mishra and Z. Y. Ma: Mater. Sci. Eng. R **50** (2005) 1–78.
17) D. Wang, B. L. Xiao, Z. Y. Ma and H. F. Zhang: Scr. Mater. **60** (2008) 112–115.